

## Effects of the 2D Semi-Circular Basin on Ground Motions Under the Incident Body Wave

KUO-LIANG WEN<sup>1</sup> and MARIJAN DRAVINSKI<sup>2</sup>

(Manuscript received 7 July 1994, in final form 15 April 1995)

### ABSTRACT

The seismic response of a sedimentary basin is especially important since many highly populated areas are located on them. The frequency responses at ground surface of the two-dimensional semi-circular basin under the incident SH-, P- and SV-waves are obtained by using the indirect boundary integral equation method. Three different incident angles ( $0^\circ$ ,  $30^\circ$  and  $60^\circ$ ) are employed in this study, while three different impedance contrast models are used in the vertical incident SH case. With an alteration in the incident angle of all waves, the amplitude and the fundamental frequency are changed accordingly. The empirical formula for the fundamental frequencies predicted by Bard and Bouchon (1985) can fit the results calculated from this semi-circular basin model at around the basin center. The transient response is constructed from the steady state solution by the Fourier synthesis. The authors use Ricker wavelets as the incident wave with three different characteristic periods (10, 5, and 3.3 in dimensionless units) to analyze the effects on the peak value and duration time. The results show the amplification effects of the peak value are very significant on the top of the basin area. The greater the impedance contrast, the more amplified the peak is, and the larger is the duration. The wavelength and incident angle of the input motion also have strong effects on the peak ground motion and duration time.

(Key words: Boundary integral equation method, Impedance contrast, Incident angle)

### 1. INTRODUCTION

Many examples show the existence of ground motion amplification on the top of an alluvium layer. Experimental studies by Ohta *et al.* (1978), Kagami *et al.* (1982, 1986), King and Tucker (1984) and Tucker and King (1984) as well as theoretical studies by Bouchon and

---

<sup>1</sup> Institute of Earth Sciences, Academia Sinica, P. O. Box 1-55, Nankang, Taipei, Taiwan, R.O.C.

<sup>2</sup> Department of Mechanical Engineering, University of Southern California, Los Angeles, CA 90089-1453, U.S.A.



Aki (1977), Bard and Bouchon (1980a, b), Dravinski (1982a, b, c; 1983), Bard and Bouchon (1985), Kawase and Aki (1989) and Dravinski *et al.* (1990) show that there appears to be a resonant type of motion in the valley that is manifested by very large amplification and duration of surface ground motion. Previous studies indicate that this resonance is not the same as that in a one-dimensional (1D) case, meaning that to realize the problem of soft basin amplification, at least two-dimensional (2D) models are required.

Scattering waves in an alluvial basin can be modeled with analytical and numerical methods although each method has its own limitations. To illustrate, the analytical method is limited to a model of very simple geometric shape. Among the numerical methods, the most commonly used, such as the finite element and finite difference methods, need discretization of the whole space. Although they can be used for more complex models, they are ineffective vis-à-vis certain problems. Another method, the boundary integral equation method, can be applied to the problem of scattering of seismic waves (Sanchez-Sesma and Rosenblueth, 1979; Dravinski, 1982a, b, c; Wong, 1982), and discretization only needs to be applied to the boundary causing the scattering (Cruse, 1968; Cole *et al.*, 1978). This procedure reduces many unknown variables and saves computer time.

The study here uses an indirect boundary integral equation method to calculate the effects of the alluvial basin on ground motion and assumes the incident plane waves are harmonic body waves. The main purpose of this paper is to study the characteristics of the ground motions at the semi-circular basin's surface under the incident body waves. The influence of the incident angle and impedance contrast are also investigated.

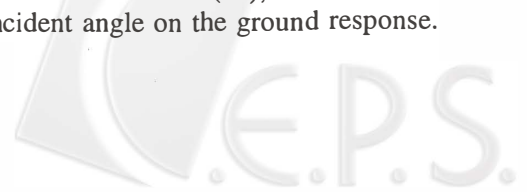
## 2. THEORETICAL MODEL AND METHOD

The numerical method used in this study is the indirect boundary integral equation method which has previously been successfully applied to geophysical and earthquake engineering problems (Sanchez-Sesma and Rosenblueth, 1979; Apsel, 1979; Dravinski, 1982a, b, c; Wong, 1982). The characteristics of this method is to introduce an auxiliary boundary to avoid the singularity problem in solving the Dynamic Green's Function. The theory behind the method and its reliability have been described in full detail by Dravinski (1982a, b, c; 1983).

The theoretical model of this study is shown in Figure 1. It is a semi-circular alluvial basin of unit radius with the material of the strata assumed to be anelastic, homogeneous and isotropic. The quality factors of the P- and S- waves are  $Q_\alpha$  and  $Q_\beta$ , respectively. In this study, it is assumed that the quality factors are the same in each domain, and  $Q_\alpha = 50$  and  $Q_\beta = 100$  are selected arbitrarily. All parameters, listed in Table 1, are in dimensionless form. Models A and C are used only in the vertical incident SH case, whereas Model B is used in each case.

## 3. STEADY STATE RESPONSE

The response of a semi-circular alluvial valley subjected to an incident plane harmonic wave is discussed in this section. The frequency responses are calculated at 101 observation points from -3 to 3 at the ground surface at 0.06 intervals. The dimensionless frequencies range from 0.01 to 1.25, and the frequency interval is 0.01. Vertical ( $0^\circ$ ),  $30^\circ$  and  $60^\circ$  incident angles are used to study the influence of the incident angle on the ground response.



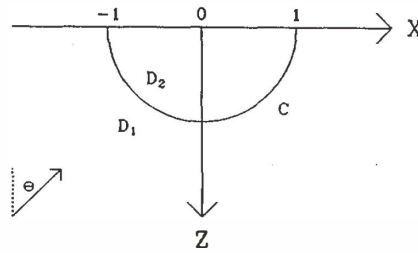


Fig. 1. The theoretical model of a semi-circular basin. Domain 1 ( $D_1$ ) is a half-space while Domain 2 ( $D_2$ ) is a semi-circular shaped alluvial basin. The P- and S-wave velocities of  $D_1$  and  $D_2$  are  $\alpha_1, \beta_1$  and  $\alpha_2, \beta_2$ , respectively. The incident wave comes from the minus X- axis direction with an angle  $\theta$ . Between  $D_1$  and  $D_2$  lies the semi-circular boundary C.

Table 1. Parameters of the three models in this study.

MODEL	DOMAIN 1			DOMAIN 2		
	$\rho_1$	$\beta_1$	$\alpha_1$	$\rho_2$	$\beta_2$	$\alpha_2$
A	1	1	—	0.8	0.6	—
B	1	1	2	0.668	0.5	1
C	1	1	—	0.6	0.4	—

$$Q_\alpha = 50, Q_\beta = 100 \text{ for each domain.}$$

To measure the influence of the impedance contrast, three different models subjected to vertically incident SH-waves are chosen. The amplitude spectrum of the data recorded at the basin center is shown in Figure 2, where it can be seen that the softer the alluvial basin is, the higher is the amplitude response.

To understand the effect of the incident angle on the steady state response, Model B subject to  $0^\circ$ ,  $30^\circ$  and  $60^\circ$  incident SH-waves is used. The results at the basin center are shown in Figure 3a. All three angles produce the same scattering effects at the basin center. Figures 3b and 3c show that the response is the same at  $x = -0.48$  and  $x = 0.48$ , respectively, and that the same frequency response as the incident angle is 0 degrees (vertical incident). This is because the model used is a symmetric basin. However, as the incident angle increases, the first mode on Figure 3b ( $x = -0.48$ ) shows a decrease in the peak amplitude, whereas in Figure 3c ( $x = 0.48$ ) it shows an increase. The focusing effects from the curvature boundary have led to this.

Figure 4a shows an example of the frequency response of the incident P wave at the basin center. The responses at the X component for the vertical incident waves are zero for all frequencies due to the cancellation of the scattered wave from the symmetric basin.

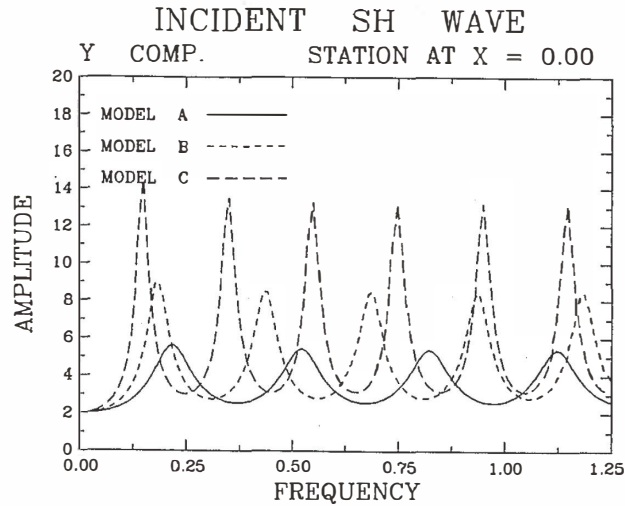


Fig. 2. The steady state response at the basin center for the three models subjected to vertically incident SH-waves.

Changing the incident angle has an effect on the amplitude as shown in Figures 3b and 3c. Figures 4b and 4c show the frequency response for the incident P-wave at  $x = -0.48$  and  $x = +0.48$  respectively. The fundamental frequency shows only a small influence from the change in the incident angle, a phenomenon which is also illustrated in Figures 3b and 3c. From a comparison of Figures 4a to 4c, it is seen that the different recording positions yield different frequency responses for the same incident wave. Different incident angles also bring about different responses. In the case of the incident SV-wave, the results are much the same as those of the incident P-wave.

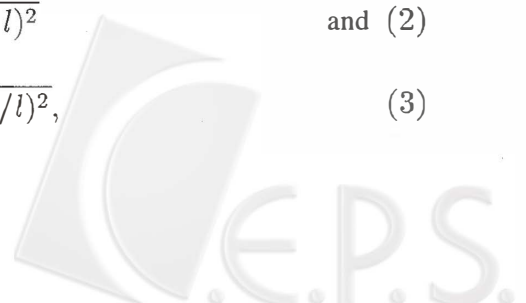
Resonance frequency is a very important parameter with which to realize the earthquake damage in an alluvium site. From Figure 2, the fundamental frequencies of Models A, B, and C are 0.23, 0.19 and 0.15, respectively. In all three cases, the values are higher than those of one-dimensional (1D) cases which are 0.15, 0.125 and 0.1, respectively ( $f_h^s = \beta/4h$ , where  $h$  is the thickness of alluvial layer). However, the relationships between 2D and 1D fundamental frequencies require further study.

A simple model of a soft rectangular inclusion was used by Bard and Bouchon (1985) to provide quantitative formulae to estimate the fundamental resonance frequencies of any valley. On the basis of their results, the empirical relations for the 2D fundamental resonance frequencies (Bard and Bouchon, 1985) are as follows:

$$f^{SH} = f_h^s \sqrt{1 + (2h/l)^2} \quad (1)$$

$$f^P = f_h^P \sqrt{1 + (h+l)^2} \quad \text{and } (2)$$

$$f^{SV} = f_h^S \sqrt{1 + (2.9h/l)^2}, \quad (3)$$



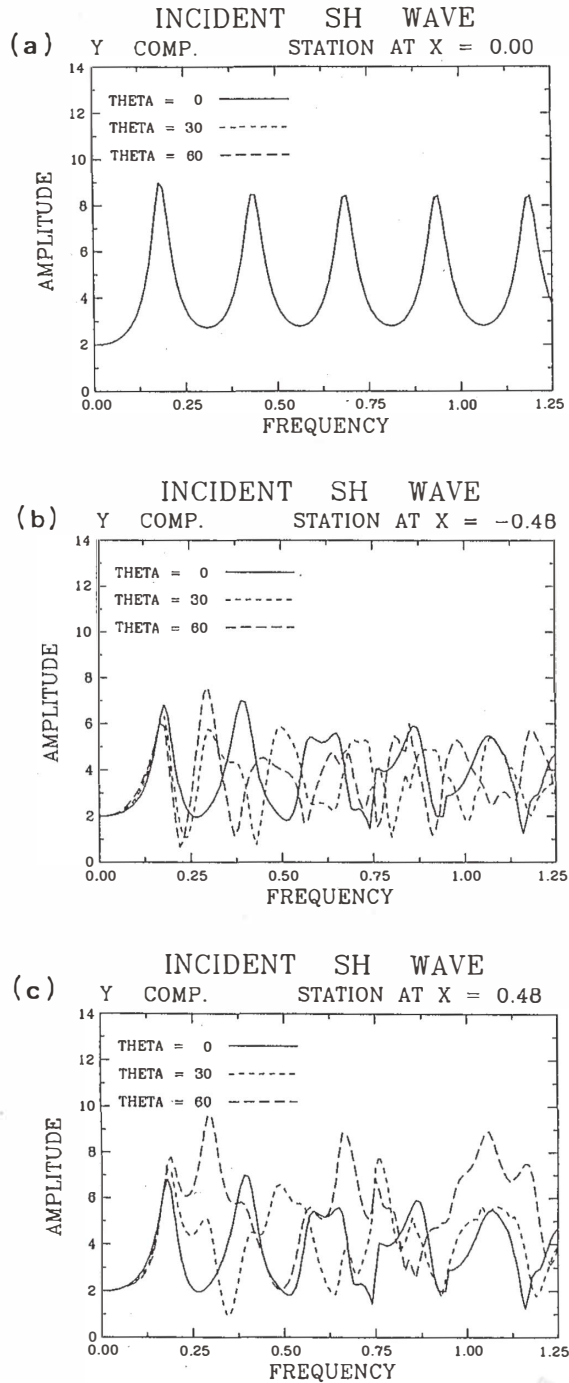


Fig. 3. The steady state response at different stations for Model B subjected to  $0^\circ$ ,  $30^\circ$  and  $60^\circ$  incident SH-waves. (a)  $x=0$ . All showing almost the same response, they appear to be only one curve here, (b)  $x=-0.48$ , and (c)  $x=0.48$ .

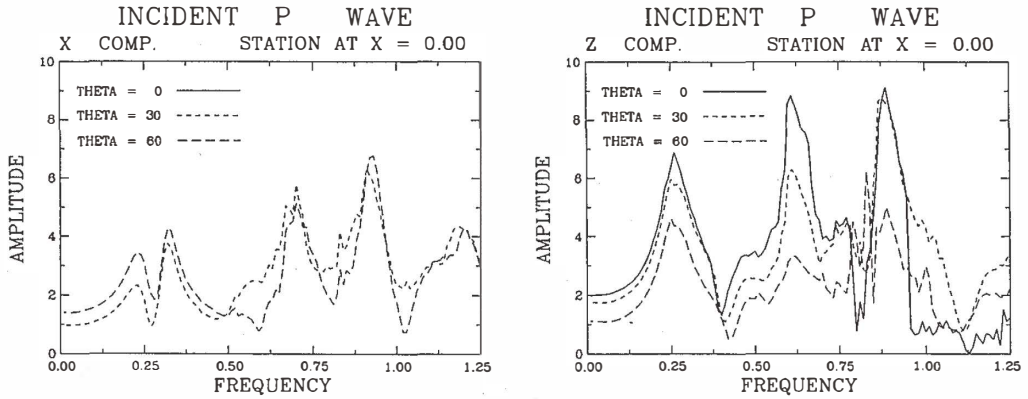


Fig. 4a. The steady state response at the basin center for various incident P-waves. As  $\theta=0^\circ$ , the basin center responds as a nodal point for the X component; all values are zero.

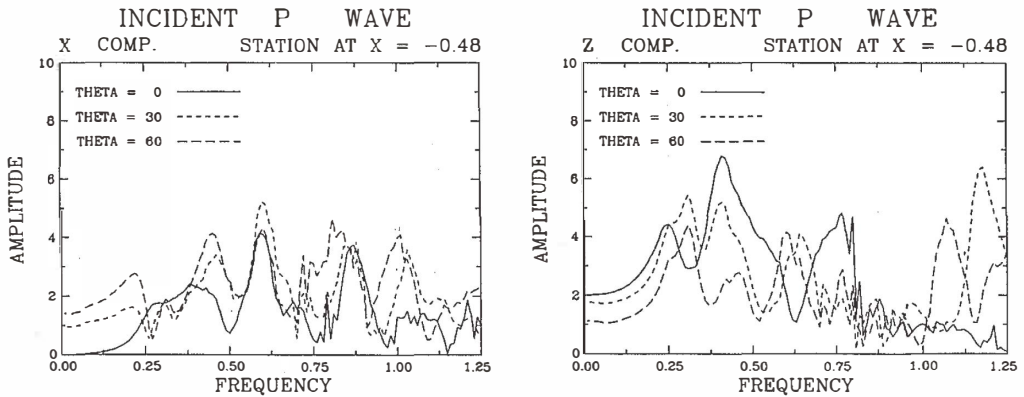


Fig. 4b. The steady state response at  $x=-0.48$  for various incident P-waves.

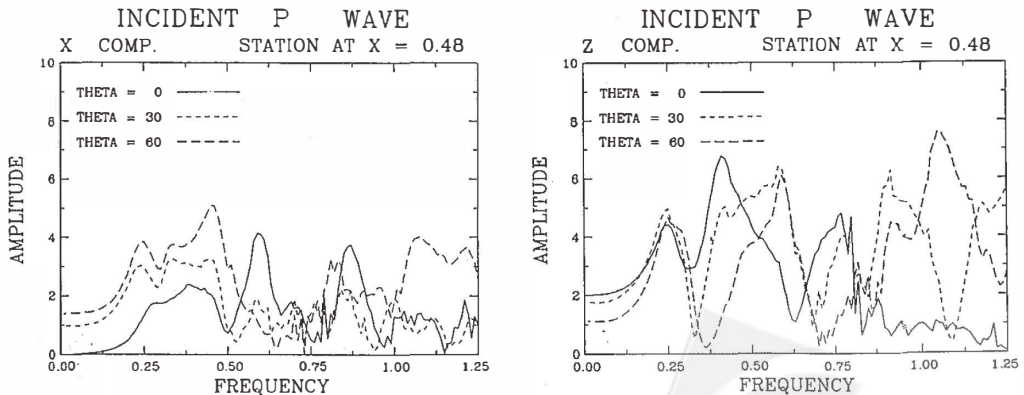
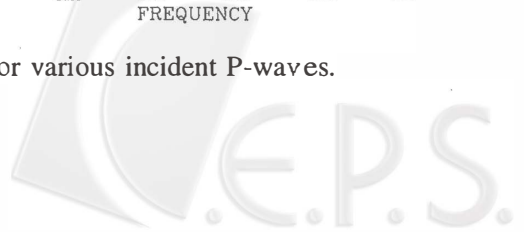


Fig. 4c. The steady state response at  $x=+0.48$  for various incident P-waves.



where  $f_h^S$  and  $f_h^P$  are the 1D fundamental frequencies of a flat layer with thickness  $h$  subjected to the incidence of the S- and P-waves respectively. The equivalent shape ratio  $h/l$  of a valley is defined as the ratio of the maximum thickness to the total width over which the valley's depth is more than one half the maximum thickness. Their estimate requires the knowledge of the two parameters: the 1D resonance frequency  $f_h$  and the shape ratio  $h/l$ . Other parameters play a very insignificant role. For the model of the semi-circular basin ( $h/l = 0.577$ ), it is found that the fundamental resonance frequencies divided by the 1D resonance frequencies in SH, P and SV cases are 1.527, 1.155 and 1.949, respectively. Figures 5a, 5b and 5c are the results of the 2D/1D fundamental frequency ratios for the incident SH-, P- and SV-waves respectively. The ratio between the 2D and 1D fundamental frequencies around the basin center coincide with the results predicted by Bard and Bouchon (1985) (represented by the thick line) in the cases of different models or different incident angles. The impedance contrast and incident angle change the ratio between the 2D and 1D fundamental frequencies very little. This parallels the conclusions reached by Bard and Bouchon (1985) exactly.

#### 4. TRANSIENT RESPONSE

To determine the variation in the peak ground motion and duration time of the ground motions, the steady state response is transferred from the frequency domain to the time domain. Ricker wavelets with 10, 5 and 3.3 dimensionless periods ( $T_p$ ) are used as input sources and convolved with previous steady state responses to obtain the transient responses at 101 observation points by the fast Fourier transform.

Figures 6a and 6b illustrate an example of the results of Model A subjected to a vertical incident plane SH-wave with 10 and 5 characteristic periods, respectively. The wavelengths ( $\lambda$ ) at the basin center in these two cases are 6 and 3, respectively. In Figure 6a, the basin radius is smaller than  $\lambda/4$ , resulting in a lack of any visible indication of resonance waves in the alluvial basin. When the wavelength decreases (Figure 6b), the resonance phenomena and reflection wave from the alluvial basin become significant. Figures 6c and 6d show the same results for Model C. The time domain responses at the basin center of Figures 6c and 6a are compared. There are resonance effects in the basin Model C (Figure 6c) which is softer than those in Model A. Based on Figure 6, it is concluded that those input waves with different characteristic periods have different basin effects. For the same incident wave, the impedance contrast of the alluvium basin also changes these effects.

In the following section, the peak value and duration time of ground motion for various input motions are examined to study the basin effects.

##### 4.1 Peak Ground Motions

To show the influences of the impedance contrast, the vertical incident SH-waves subjected to three models are used. Figure 7 shows the three different impedance contrast models subjected to vertical incident SH Ricker wavelets with the three characteristic periods. This figure illustrates the significant peak amplification effects in the alluvial basin area ( $-1 < x < 1$ ). The greater the impedance contrast, the larger the amplification of the peak is. Meanwhile, the thicker the alluvial layer (near the basin center), the larger the amplification of the peak is for the same model. The peak amplification also shows slight differences between the various characteristic periods (or dominate frequencies) of the incident waves for the same model. This means that the peak amplification not only is affected by site effects but it also dominates the frequencies of the incident waves.

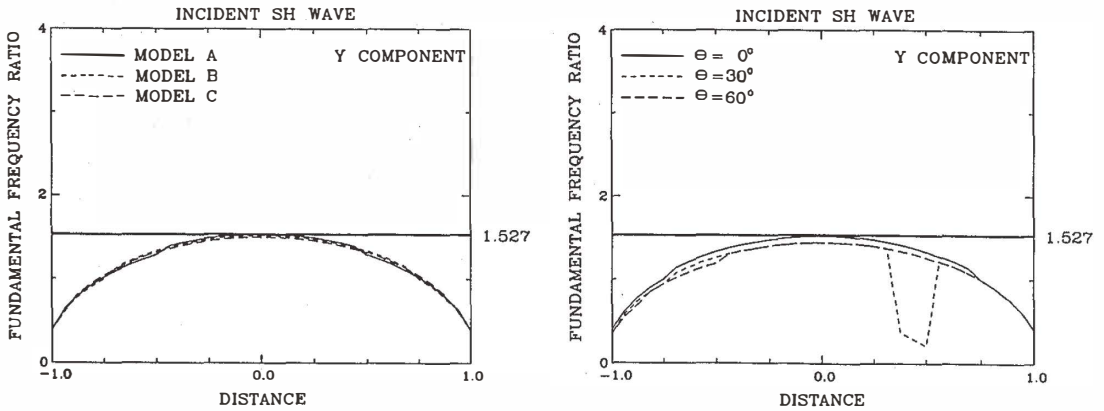


Fig. 5a. The fundamental frequency ratios. The top map is the result of the three models subjected to a vertical incident SH-wave, while the lower map shows Model B subjected to SH-waves in three incident angles. The thick line shows the value predicted by Bard and Bouchon (1985).

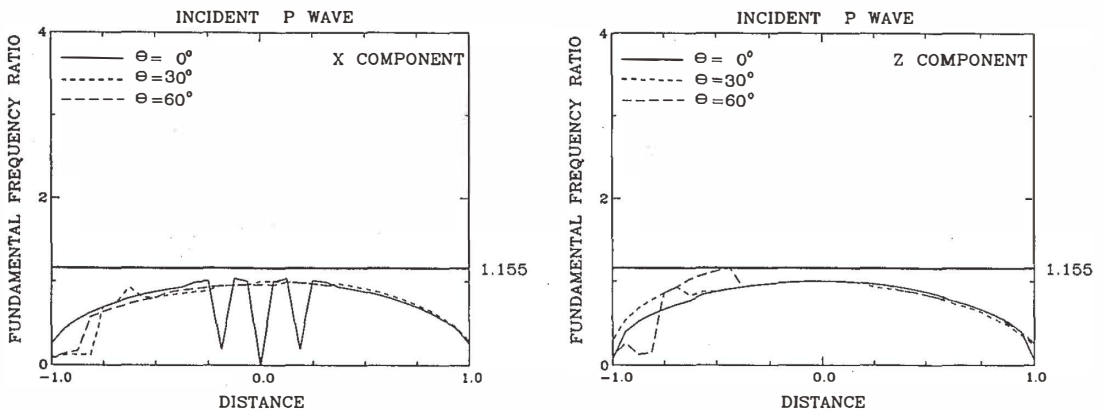


Fig. 5b. The fundamental frequency ratios for various incident P-waves. The thick line shows the value predicted by Bard and Bouchon (1985).

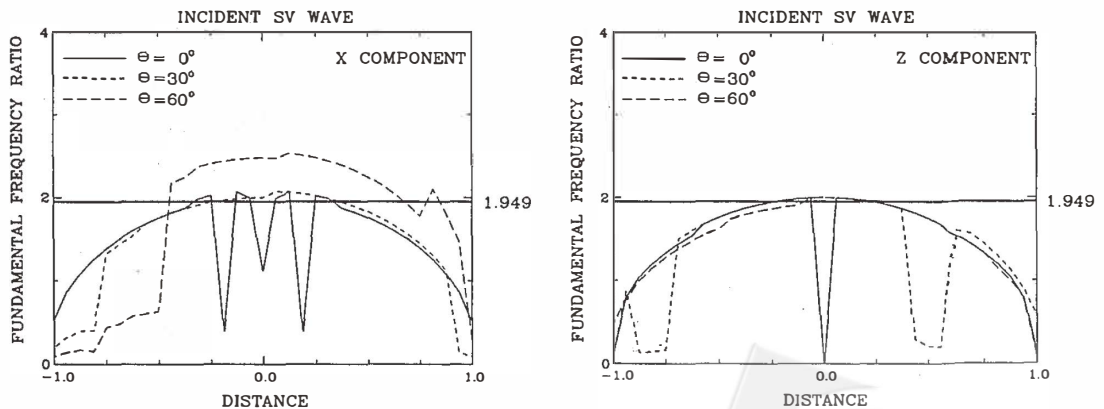
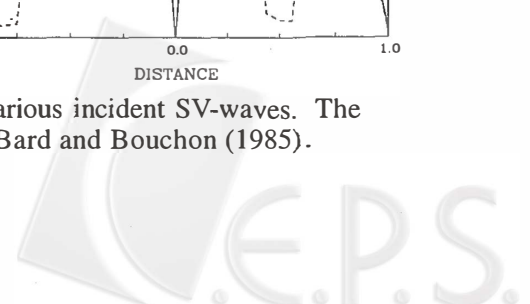


Fig. 5c. The fundamental frequency ratios for various incident SV-waves. The thick line shows the value predicted by Bard and Bouchon (1985).





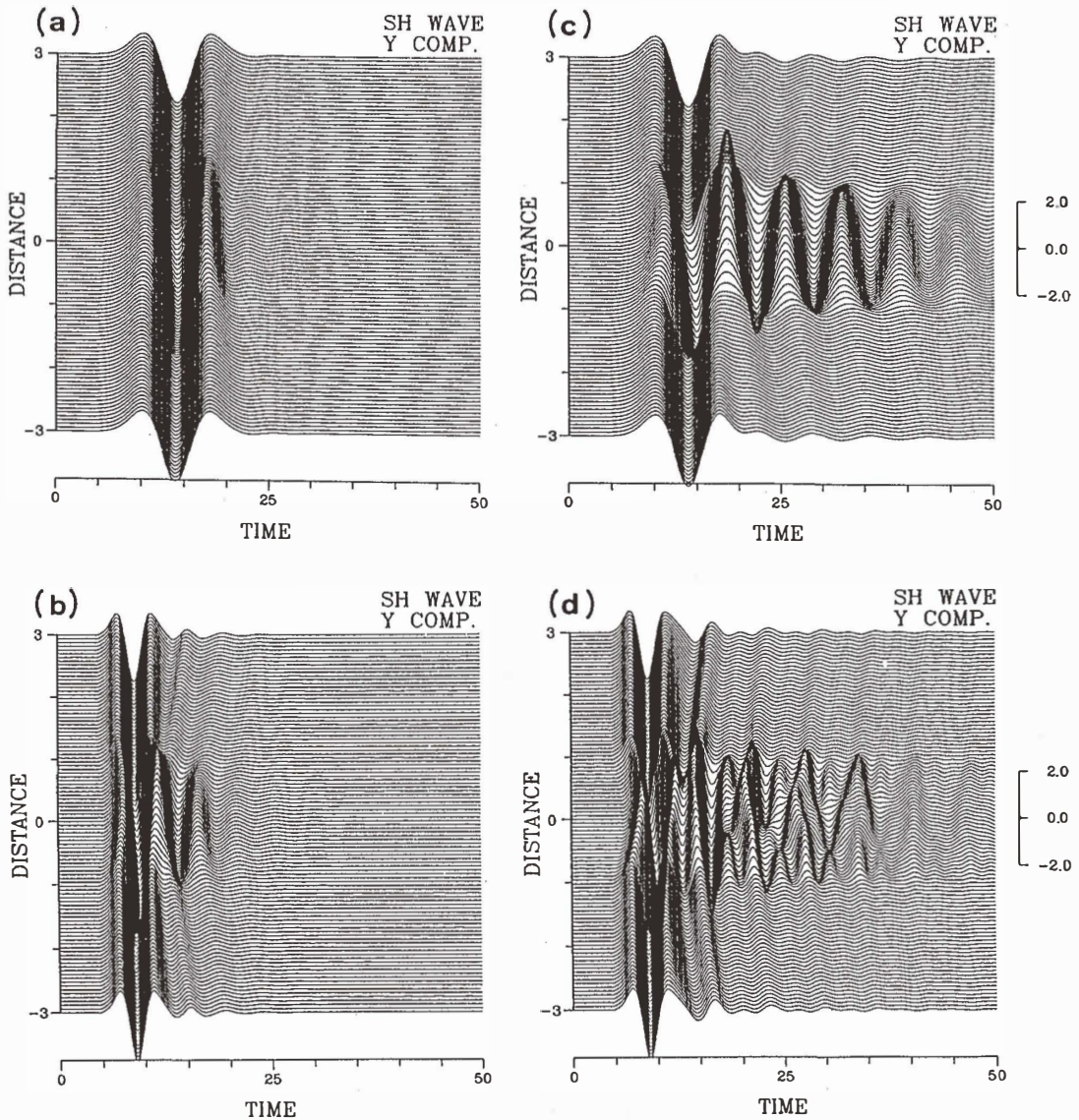


Fig. 6. The transient response of two models subjected to a vertical incident SH Ricker wavelet with two characteristic periods: (a) Model A and  $T_p=10$ , (b) Model A and  $T_p=5$ , (c) Model C and  $T_p=10$ , and (d) Model C and  $T_p=5$ .

To investigate the influences of the incident angle, Model B subjected to three different incident angles of the SH-wave is used. The ratio between the peak of each trace and the peak of the incident wave is shown in Figure 8. On the top of the basin area, the amplification effect of the peak is still very significant. The incident angle does not significantly affect the peak amplitude of the motion (in Figure 8a). From Figures 8b and 8c, it can be seen that the incident angle affects the peak amplitude of the motion and that the peak location has been

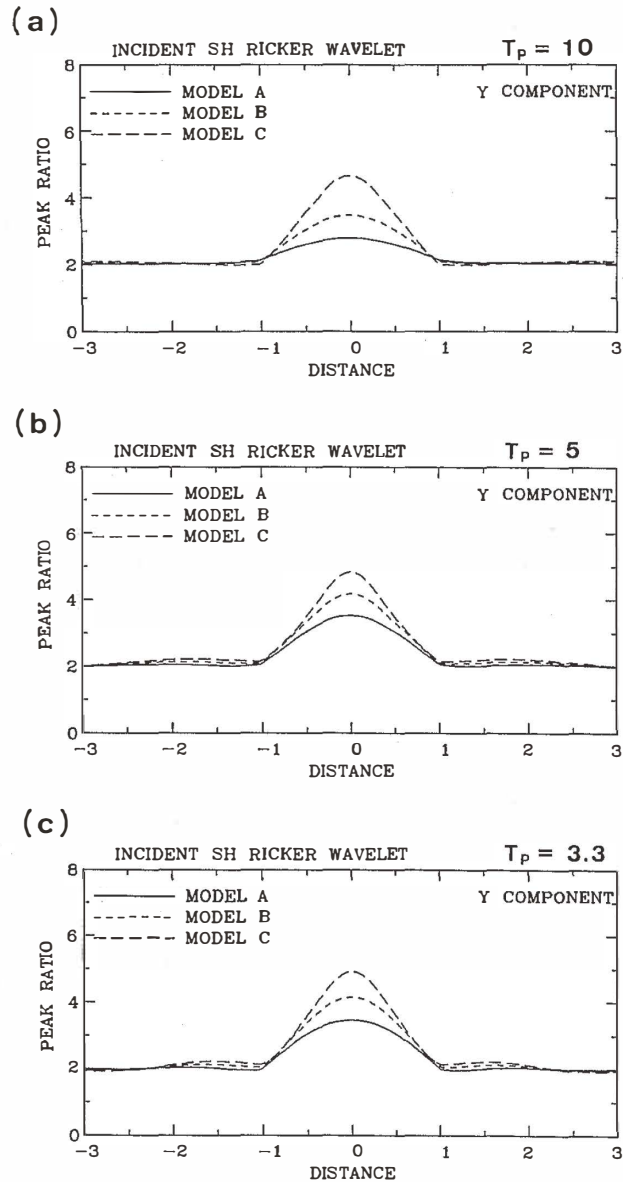


Fig. 7. The peak amplification ratios of the three models subjected to a vertical incident Ricker wavelet with three characteristic periods: (a)  $T_p=10$ , (b)  $T_p=5$ , and (c)  $T_p=3.3$ .

shifted to the right side of the basin center. This is due to the wave incident from the minus X direction. Outside the alluvial basin ( $x < -1$ ), the peak ground motion is only slightly amplified. However, the results on the right hand side demonstrate a slight deamplification effect. In fact, the greater the incident angle, the larger is the area deamplified. This may be explained by the shadow effects of the basin. From this study, it is understood that the rock site near an alluvium basin may already be influenced by the basin effect.

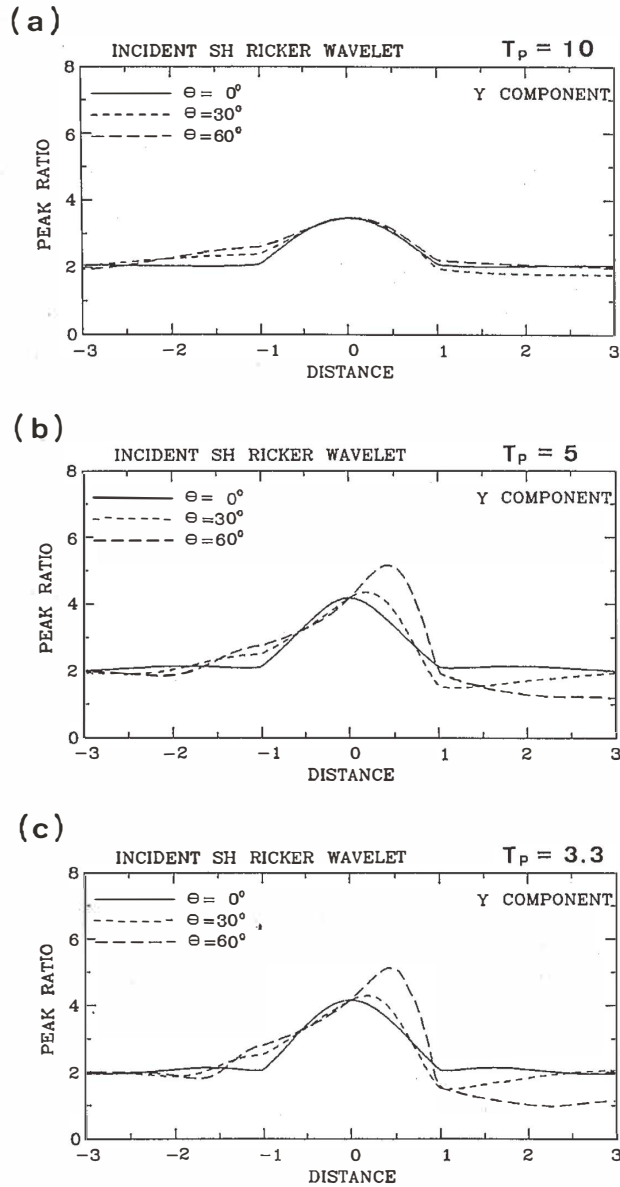


Fig. 8. The peak amplification ratios of Model B subjected to  $0^\circ$ ,  $30^\circ$  and  $60^\circ$  incident Ricker wavelets with three characteristic periods: (a)  $T_p=10$ , (b)  $T_p=5$ , and (c)  $T_p=3.3$ .

#### 4.2 Duration Time

The duration of strong ground shaking may play a significant role in the damage caused by an earthquake, and thus, is an important factor which needs to be considered in many earthquake engineering problems. Since no single quantitative measure of duration is in common usage in earthquake engineering, a simple measure of duration is used in this study. Based on the concept of cumulative energy obtained by integrating squared ground

motions, duration is defined as the time interval required to accumulate 90% of the total energy (Trifunac and Brady, 1975), and the duration ratio is defined as the ratio between the duration at the ground surface and that of the input motion.

The effects of the impedance contrast and incident angle on the duration time are determined in this part of the study. The duration ratios for the three models subjected to vertical incident SH-waves with three different periods are shown in Figure 9. It can be found that the larger the impedance contrast is, the longer is the duration time. A comparison among

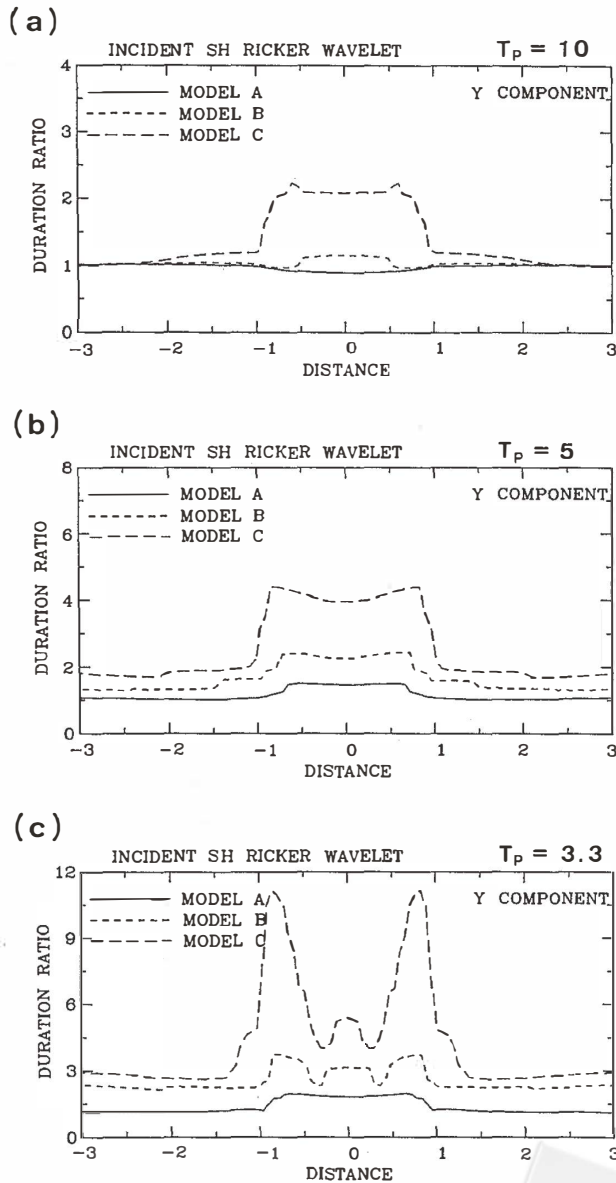


Fig. 9. The duration elongation ratios of three models subjected to a vertical incident Ricker wavelet with three characteristic periods: (a)  $T_p=10$ , (b)  $T_p=5$ , and (c)  $T_p=3.3$ .

Figures 9a - 9c shows that the incident wavelength and the location of the observations have even greater effects on the elongation of the duration time.

Figure 10 presents the results of the duration ratio of Model B subjected to different incident angles of the SH-wave. Figure 10a shows that the duration only elongates a little as the quarter wavelength of the incident wave becomes greater than the radius of the basin. On the other hand, the duration ratios increase slightly as the incident angle increases on the left hand side of the basin center ( $-1 < x < 0$ ), whereas they decrease on the right hand side

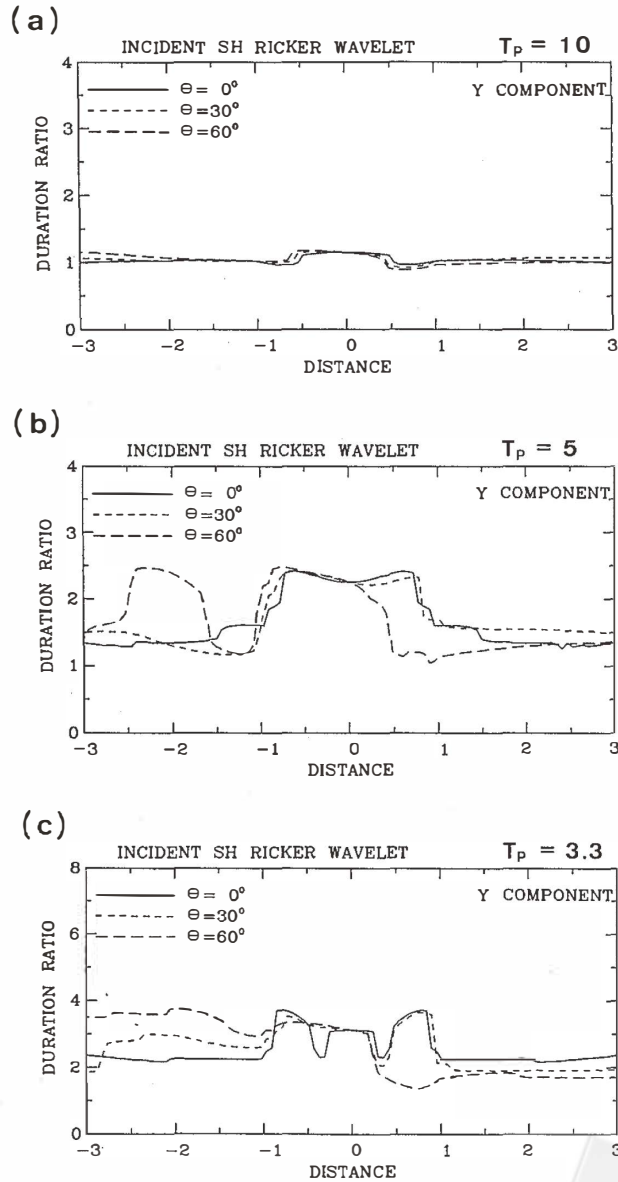


Fig. 10. The duration elongation ratios of Model B subjected to  $0^\circ$ ,  $30^\circ$ , and  $60^\circ$  incident Ricker wavelets with three characteristic periods: (a)  $T_p=10$ , (b)  $T_p=5$ , and (c)  $T_p=3.3$ .

( $0 < x < 1$ ). The position of the peak ratio shifts from the basin center to the edge when the characteristic period decreases in the vertical incident case, showing the wavelengths of the input wave also affect the duration time. Comparing the results of the different incident angles, it can be found that though the duration ratios increase on the left hand side of the basin ( $x < -1$ ), they do so mostly at 60 degrees. The reason for this is the scatter wave generated by the soft basin boundary. The results for the incident P- and SV-waves have the same features. The incident wavelength also influences the extension of the duration time. The duration ratio in the basin area become larger as the characteristic period of the incident wave changes from 10 to 3.3.

## 5. SUMMARY

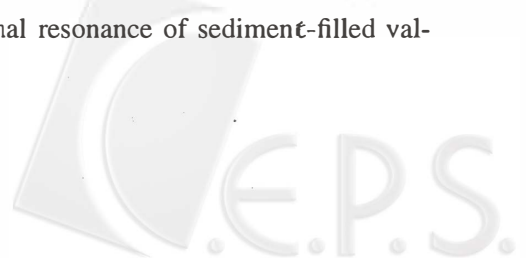
The effects of a two-dimensional semi-circular basin on ground motions under the incident plane SH-, P- and SV- waves are studied by using the indirect boundary integral equation method. Three different incident angles,  $0^\circ$ ,  $30^\circ$  and  $60^\circ$  are used in this study. The steady state results show that the incident angle changes the amplitude and fundamental frequency for all P-, SV- and SH-waves. The fundamental frequency is also altered as the incident angle changes. The resonance frequencies predicted from the empirical formulae, obtained by Bard and Bouchon (1985), can suit the results of the semi-circular basin model near the basin center.

The frequency response is convolved with different characteristic periods of Ricker wavelets and converted to the time domain through the Fourier transform method. From the transient response, the variations in peak ground motion and duration time are studied. Additionally, the influences of the impedance contrast and incident angle are analyzed. From this study, it is noted that the peak ground motion and duration time vary according to station positions and observation components of the observation site, wave types, dominant frequencies and the incident angle of the input motion.

**Acknowledgments** This work was supported by the Institute of Earth Sciences, Academia Sinica, the National Science Council of the R.O.C. and the National Science Foundation of the U.S.A. under NSF Grant INT- 9021623. The authors thank the Computer Center of Academia Sinica for use of the ETA-10Q supercomputer. They are also grateful to two anonymous reviewers for their constructive comments.

## REFERENCE

- Apsel, R. J., 1979: Dynamic Green's functions for layered media and application to boundary value problems. Ph. D. Thesis, University of California at San Diego.
- Bard, P.-Y., and M. Bouchon, 1980a: The seismic response of sediment-filled valleys. Part I: The case of incident SH waves. *Bull. Seism. Soc. Am.*, **70**, 1263-1286.
- Bard, P.-Y., and M. Bouchon, 1980b: The seismic response of sediment-filled valleys. Part II: The case of incident P and SV waves. *Bull. Seism. Soc. Am.*, **70**, 1921-1941.
- Bard, P.-Y., and M. Bouchon, 1985: The two dimensional resonance of sediment-filled valleys. *Bull. Seism. Soc. Am.*, **75**, 519-541.



- Bouchon, M., and K. Aki, 1977: Near field of a seismic source in a layered medium with irregular interfaces. *Geophys. J. R. Astr. Soc.*, **50**, 3, 669-684.
- Cole, D. M., D. D. Kosloff, and J. B. Minster, 1978: A numerical boundary integral equation method for elasto-dynamics. *Bull. Seism. Soc. Am.*, **68**, 1331-1357.
- Cruse, T. A., 1968: A direct formulation and numerical solution of the general transient elastodynamic problem, II. *J. Math. Anal. Appl.*, **22**, 341-355.
- Dravinski, M., 1982a: Influence of interface depth upon strong ground motion. *Bull. Seism. Soc. Am.*, **72**, 596-614.
- Dravinski, M., 1982b: Scattering of SH waves by subsurface topography. *J. Eng. Mech. Div.*, **108**, 1-16.
- Dravinski, M., 1982c: Scattering of elastic waves by an alluvial valley. *J. Eng. Mech. Div.*, **108**, 19-31.
- Dravinski, M., 1983: Scattering of plane harmonic SH waves by dipping layers of arbitrary shape. *Bull. Seism. Soc. Am.*, **73**, 1303-1319.
- Dravinski, M., T. K. Mossessian, H. Eshraghi, and H. Kagami, 1990: Predominant motion of the Los Angeles sedimentary basin. *Eng. Anal. Bound. Elem.*, **8**, 206-214.
- Kagami, H., C. M. Duke, G. C. Liang, and Y. Ohta, 1982: Observation of 1- to 5-second microtremors and their application to earthquake engineering. Part II: Evaluation of site effect upon seismic wave amplification due to extremely deep soil deposits. *Bull. Seism. Soc. Am.*, **72**, 987-998.
- Kagami, H., S. Okada, K. Shiono, M. Oner, M. Dravinski, and A. Mal, 1986: Observation of 1- to 5-second microtremors and their application to earthquake engineering. Part III: A two dimensional study of site effect in the San Fernando valley. *Bull. Seism. Soc. Am.*, **76**, 1801-1812.
- Kawase, H., and K. Aki, 1989: A study on the response of a soft basin for incident S, P, and Rayleigh waves with special reference to the long duration observed in Mexico City. *Bull. Seism. Soc. Am.*, **79**, 1361-1382.
- King, J. L., and B. E. Tucker, 1984: Observed variations of earthquake motion across a sediment-filled valley. *Bull. Seism. Soc. Am.*, **74**, 137-151.
- Kobayashi, S., 1983: Some problems of the boundary integral equation method in elastodynamics. Proc. Fifth Int'l Conference in Boundary Elements, Hiroshima, Japan, In: C. A. Brebbia, T. Futagami, and M. Tanaka (Eds.), Springer-Verlag, New York, 775-784.
- Ohta, Y., H. Kagami, N. Goto, and K. Kudo, 1978: Observation of 1- to 5- second microtremors and their application to earthquake engineering. Part I: Comparison with long-period accelerations at the Tokachi-oki earthquake of 1968. *Bull. Seism. Soc. Am.*, **68**, 767-779.
- Sanchez-Sesma, F. J., and E. Rosenblueth, 1979: Ground motion of canyons of arbitrary shapes under incident SH-waves. *Earthq. Eng. Struct. Dyn.*, **7**, 441-449.
- Trifunac, M. D., and A. G. Brady, 1975: A study on the duration of strong earthquake ground motion. *Bull. Seism. Soc. Am.*, **65**, 581-626.
- Tucker, B. E., and J. L. King, 1984: Dependence of sediment-filled valley response on the input amplitude and the valley properties. *Bull. Seism. Soc. Am.*, **74**, 153-165.
- Wong, H. L., 1982: Diffraction of P, SV, and Rayleigh waves by surface topographies. *Bull. Seism. Soc. Am.*, **72**, 1167-1184.

